

REPORT DOCUMENTATION PAGE

Form Approved
OMB No. 0704-0188

Public reporting burden for this collection of information is estimated to average 1 hour per response, including the time for reviewing instructions, searching existing data sources, gathering and maintaining the data needed, and completing and reviewing this collection of information. Send comments regarding this burden estimate or any other aspect of this collection of information, including suggestions for reducing this burden to Department of Defense, Washington Headquarters Services, Directorate for Information Operations and Reports (0704-0188), 1215 Jefferson Davis Highway, Suite 1204, Arlington, VA 22202-4302. Respondents should be aware that notwithstanding any other provision of law, no person shall be subject to any penalty for failing to comply with a collection of information if it does not display a currently valid OMB control number. **PLEASE DO NOT RETURN YOUR FORM TO THE ABOVE ADDRESS.**

1. REPORT DATE (DD-MM-YYYY)		2. REPORT TYPE Published Journal Article		3. DATES COVERED (From - To) January 2003- October 2008	
4. TITLE AND SUBTITLE TRENDS IN RETINAL DAMAGE THRESHOLDS FROM CONTINUOUS-WAVE NEAR-IR LASER ADIATION: A STUDY AT 1110, 1130, 1150, 1139 NM				5a. CONTRACT NUMBER F41624-02-D-7003	
				5b. GRANT NUMBER	
				5c. PROGRAM ELEMENT NUMBER 63231F	
6. AUTHOR(S) Rebecca Vincelette, Benajmin Rocksell, Jeff Oliver, Semih Kumru, Robert Thomas, Kurt Schuster, Gary Noojin, Aurora Shingledecker, Dave Stolarski, Ashley Welch				5d. PROJECT NUMBER 7757	
				5e. TASK NUMBER B2	
				5f. WORK UNIT NUMBER 26	
7. PERFORMING ORGANIZATION NAME(S) AND ADDRESS(ES) Air Force Research Laboratory Human Effectiveness Directorate Directed Energy Bioeffects Division Optical Radiation Branch 2624 Louis Bauer Dr. Brooks City-Base, TX 78235-5128				8. PERFORMING ORGANIZATION REPORT NUMBER	
9. SPONSORING / MONITORING AGENCY NAME(S) AND ADDRESS(ES) Air Force Research Laboratory Human Effectiveness Directorate Directed Energy Bioeffects Division Optical Radiation Branch 2624 Louis Bauer Dr. Brooks City-Base, TX 78235-5128				10. SPONSOR'S/MONITOR'S ACRONYM(S) AFRL/RHDO	
				11. SPONSOR'S/MONITOR'S REPORT NUMBER(S) AFRL-HE-BR-JA-2008-0025	
12. DISTRIBUTION / AVAILABILITY STATEMENT APPROVED FOR PUBLIC RELEASE; DISTRIBUTION UNLIMITED. Case file no. 09-002, 5 Jan. 09 Published in Lasers in Surgery and Medicine 41:382-390 (2009)					
13. SUPPLEMENTARY NOTES					
14. ABSTRACT Retinal damage thresholds from 100-millisecond exposures to laser radiation for wavelengths between 1,100 and 1,350nm have never previously been established. We sought to determine the retinal damage threshold for 100-millisecond exposures of near-infrared (NIR) laser radiation wavelengths at 1,110, 1,130, 1,150, and 1,319 nm. These data were then used to create trends for retinal damage thresholds over the 1,100–1,350nm NIR region based upon linear absorption of laser radiation in ocular media and chromatic dispersion of the eye.					
15. SUBJECT TERMS eye safe; laser safety; laser tissue interaction; non-ionizing radiation; ocular hazard					
16. SECURITY CLASSIFICATION OF:			17. LIMITATION OF ABSTRACT UU	18. NUMBER OF PAGES 10	19a. NAME OF RESPONSIBLE PERSON 19b. TELEPHONE NUMBER (include area code)
a. REPORT Unclassified	b. ABSTRACT Unclassified	c. THIS PAGE Unclassified			

Trends in Retinal Damage Thresholds From 100-millisecond Near-Infrared Laser Radiation Exposures: A Study at 1,110, 1,130, 1,150, and 1,319 nm

Rebecca L. Vincelette, MS,^{1*} Benjamin A. Rockwell, PhD,² Jeff W. Oliver, PhD,² Semih S. Kumru, PhD,² Robert J. Thomas, PhD,² Kurt J. Schuster, MS,³ Gary D. Noojin, AAS,³ Aurora D. Shingledecker, CVA,³ Dave J. Stolarski, BA,³ and Ashley J. Welch, PhD¹

¹Department of Biomedical Engineering, Cockrell School of Engineering, University of Texas, 1 University Station, C0800, Austin, Texas 78712

²Air Force Research Laboratory, 711th HPW, Optical Radiation Branch, 2624 Louis Bauer Dr., Brooks City-Base, Texas 78231

³Northrop Grumman, 4241 Woodcock Dr. Ste. B-100, San Antonio, Texas 78228

Background and Objectives: Retinal damage thresholds from 100-millisecond exposures to laser radiation for wavelengths between 1,100 and 1,350 nm have never previously been established. We sought to determine the retinal damage threshold for 100-millisecond exposures of near-infrared (NIR) laser radiation wavelengths at 1,110, 1,130, 1,150, and 1,319 nm. These data were then used to create trends for retinal damage thresholds over the 1,100–1,350 nm NIR region based upon linear absorption of laser radiation in ocular media and chromatic dispersion of the eye.

Materials and Methods: The paramacula and macula areas of the retina in *Macaca mulatta* (rhesus) subjects were exposed for 100 milliseconds to NIR laser radiation wavelengths using a Coherent OPO laser for 1,110, 1,130, and 1,150 nm and a Lee laser for 1,319 nm. Probit analysis was used to establish the estimated damage threshold in the retina for 50% of exposures (ED₅₀). Using trends of transmitted energy to the retina, refractive error of the eye and linear absorption of the retina, a scaling factor (SF) method was created to fit the experimental data, predicting retinal damage thresholds over the 1,100–1,350 nm region.

Results: The experimental retinal damage threshold, ED₅₀, for 100-millisecond exposures for laser radiation wavelengths at 1,110, 1,130, and 1,319 nm were determined to be 193, 270, and 13,713 mW of power delivered to the cornea, respectively. The retinal damage threshold for the 1,150 nm wavelength was statistically undetermined due to laser-power limitations, but was achieved in one out of three subjects tested.

Conclusion: The SF predicts the experimental 100-millisecond NIR ED₅₀ value for wavelengths between 1,100 and 1,350 nm. *Lasers Surg. Med.* 41:382–390, 2009. © 2009 Wiley-Liss, Inc.

Key words: eye safe; laser safety; laser tissue interaction; non-ionizing radiation; ocular hazard

INTRODUCTION

The near-infrared (NIR) laser radiation region between 1,150 and 1,350 nm is a unique area in the electromagnetic spectrum for laser safety. It is in this region, where ocular media begins to absorb very strongly, but still transmits sufficient energy to pose a hazard to the retina. Retinal damage threshold studies are conducted at specific laser radiation parameters to quantify these hazards. These studies are then analyzed by international safety committees such as the American National Standards Institute (ANSI) and the International Commission of Non-Ionizing Radiation Protection (ICNIRP) for making recommendations for safe exposure levels [1,2].

For 100-millisecond laser radiation exposures, the retinal damage threshold data are a function of three fundamental physical characteristics: (1) the transmission of laser radiation to the retina, (2) absorption of laser radiation by the retina, and (3) the diameter of the laser-spot formed at the retina [3]. The diameter of the laser-spot formed at the retina is typically taken to be dependent on the natural chromatic dispersion properties of the eye, independent of absorption and thermal properties of the tissue.

NIR 1,300-nm laser radiation retinal damage thresholds have been conducted by the United States Army and Air Force over the past several decades. Retinal lesion studies conducted on *Macaca mulatta* and rabbit subjects at 1,318 nm discovered that lesions could be placed on a rabbit's retina regardless of exposure duration, but could only be placed in a non-human primate's retina for exposures less than 1 millisecond [4–8]. This discrepancy in the occurrence of retinal lesions between species has

Contract grant sponsor: Air Force Research Laboratory; Contract grant number: FA8650-05-2-6501.

*Correspondence to: Rebecca L. Vincelette, MS, 109 Blue Sage Ln., Cibolo, TX 78108. E-mail: rebecca.vincelette@gmail.com

Accepted 7 April 2009

Published online in Wiley InterScience
(www.interscience.wiley.com).

DOI 10.1002/lsm.20772

never been observed in the previous 40 years of testing, leaving retinal damage threshold studies on the conventional *M. mulatta* animal models for 100-millisecond exposures to NIR laser radiation inconclusive at 1,318 nm. Additionally, retinal damage studies in the laser radiation region of 1,100–1,300 nm wavelengths have not been conducted for 100-millisecond exposures.

This article presents data from a retinal damage threshold study using 100-millisecond exposures to 1,110, 1,130, 1,150, and 1,319 nm laser radiation wavelengths. The paramacula was exposed for laser radiation wavelengths of 1,110, 1,130, and 1,150 nm, while the macula was used for the 1,319 nm study. These data are compared to trends in the three fundamental criteria previously mentioned.

BACKGROUND

In the 1,318 nm NIR laser radiation retinal damage threshold studies conducted in rabbits by Zuclich et al. [4,5,9], lesions were never apparent after 1-hour post-exposure, but were seen after 24 hours. In other laser radiation retinal damage studies, below 1,100 nm, a small number of lesions appeared at the 24-hour end point, but the majority (> 90%) of lesions were present at 1 hour [10]. Histology of the 1,318-nm radiation lesions also revealed full-retinal thickness damage at threshold level energies, a trait seen in visible lesions only for suprathreshold exposures [5]. Zuclich et al. [5] also reported that lesions which appeared at 24 hours increased, even doubling, in size, stabilizing after 48 hours post-exposure. Again, extensive growth in lesion size is not a characteristic trait for lesions caused by visible laser radiation wavelengths. Though histology is not provided for the study presented here, these observations from Zuclich et al. [4,5,9] provide a basis for understanding our data.

Lund et al. have created an action spectrum to fit retinal damage threshold data using three fundamental criteria of transmission, absorption, and radius, subject to chromatic dispersion, of the laser radiation reaching the retina [3,11–14]. The transmission of NIR laser radiation from the cornea to the retina in a rhesus and human was predicted using one-dimensional Beer's law and linear absorption data from Maher [15]. Physical thicknesses for the cornea, aqueous humor, crystalline lens, and vitreous humor were obtained from Fernandes et al. [16], Li et al. [17], and Westheimer [18]. The percent transmission decreases sharply, as indicated in Figure 1, for the three wavelengths of 1,110, 1,130, and 1,150 nm from 57.3% to 42.2% and finally 12.4%, respectively, in the rhesus eye. The percent of laser radiation transmitted at 1,319 nm for a rhesus eye is ~3%. The total absorption of the pre-retinal media can be estimated from Figure 1 by subtracting the percent transmission from 100% (this neglects reflection).

Lund et al. [14] determined the retinal pigment epithelium (RPE) laser radiation absorption data which provided the best-fit to retinal damage threshold data were from Gabel et al. [19] and Birngruber et al. [20] where the percent of laser radiation reaching the retina is absorbed by the neural retina and RPE at 1,110, 1,130, 1,150, and 1,319 nm wavelengths is 3.87%, 3.55%, 3.26%, and 1.58%,

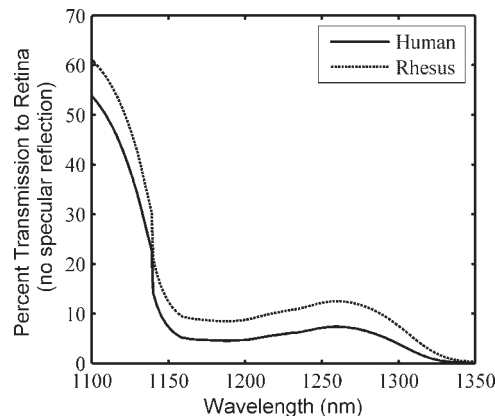


Fig. 1. Transmission of laser radiation in a human and rhesus eye based on linear absorption data of Maher [15]. These results assumed physical thicknesses of the cornea, aqueous humor, crystalline lens, and vitreous humor from Fernandes et al. [16], Li et al. [17], and Westheimer [18].

respectively. Note the variability between the 1,110, 1,130, and 1,150 nm wavelengths is less than 1%, but the 1,319 nm wavelength is about a factor of 2.25 times smaller (Table 1). Birngruber et al. [20] compared the histological sections of a monkey's retina for several subjects, reporting that the average thickness of the layer of pigmented granules which are found in the cells of the RPE is approximately 5 μm . Birngruber et al. reported finding equivalent pigmentations in the RPE and choroid with pigmentation distributed throughout the choroid (no pigmentation was reported in the choriocapillaris). From their histological findings, Birngruber et al. [20] reported the absorption coefficient, μ_a , of the RPE to be the same for the pigmented regions of the choroid. Here, we are assuming that this absorption coefficient for the RPE and choroid reported by Birngruber et al. includes water absorption, and thus assume these values account for any absorption which would occur in the neural retina. The μ_a for RPE over wavelengths from 1,000 to 1,400 nm is shown in Figure 2. The exponential fit to the absorption coefficients, μ_a (cm^{-1}), for wavelength, λ (nm), in rhesus RPE is

$$\mu_a(\lambda) = 15874 * \exp(-4.59 * 10^{-3}\lambda) \quad (1)$$

When a collimated beam is normal to the cornea, it is focused by the cornea and lens. The $1/e^2$ laser-spot diameter formed on the retina (Fig. 3) by chromatic dispersion was

TABLE 1. The Linear Absorption Coefficient of the RPE, μ_a , for the Laser Radiation Wavelengths in This Study

(nm)	μ_a (cm^{-1})
1,110	97.87
1,130	89.30
1,150	81.48
1,319	37.54

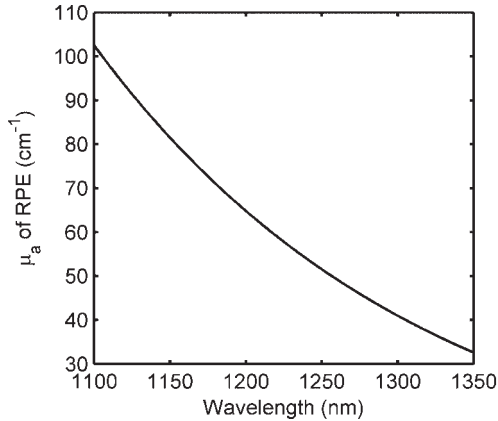


Fig. 2. Absorption by retinal pigment epithelium (RPE) based on a fit to data from Birngruber et al. [20].

determined by superimposing refractive error measurements of human eyes onto a simple rhesus eye model [3]. The predicted diameter formed at the rhesus retina for laser radiation wavelengths of 1,110, 1,130, and 1,150 nm is 146.5, 150.6, and 153.8 μm respectively. The variability between these three wavelengths' laser-spot diameter due to chromatic dispersion is less than 5%. In Figure 3, the laser-spot diameter for the 1,319-nm wavelength is approximately 184.6 μm , or approximately 25% larger than the other three laser radiation wavelengths in this study.

Of the three fundamental criteria leading to retinal damage from laser radiation presented in Figures 1–3, the transmitted energy is by far the distinguishing variable between 1,110, 1,130, and 1,150 nm wavelengths. For these three wavelengths, the absorption of the RPE and the laser-spot diameter delivered to the retina vary by less than 1% and 5%, respectively. However, the 1,319 nm laser radiation wavelength is considerably different from the 1,110,

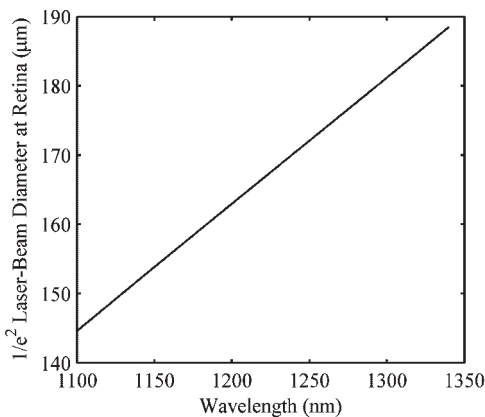


Fig. 3. The $1/e^2$ laser-spot diameter for NIR laser radiation wavelengths delivered to the rhesus retina with chromatic dispersion. Results shown here are based upon a collimated beam with a 4.24-mm $1/e^2$ diameter delivered to the corneal plane.

1,130, and 1,150 nm wavelengths with respect to each of the three fundamental criteria.

MATERIALS AND METHODS

The subjects in this study were four adult, male rhesus (*M. mulatta*), approximately 4–5 years in age. Animals used in this study were procured, maintained, and used in accordance with the Animal Welfare Act and the “Guide for the Care and Use of Laboratory Animals” prepared by the Institute of Laboratory Animal Resources, National Research Council; and the ARVO Resolution on the Use of Animals in Research. Subjects were screened for any ocular defects prior to beginning the study. Subjects were chemically restrained with intramuscular injections of Telazol (5–10 mg/kg body mass). Subjects then received a subcutaneous injection of 0.16 mg atropine sulfate and eye drops; two drops each of proparacaine hydrochloride 0.5%, phenylephrine hydrochloride 2.5%, and tropicamide 1%, to dilate the eye. Bilateral saphenous catheters were used both for administering anesthetic (Propoflo[®] 1,500 Mcg/kg bolus, then continuous rate infusion at 300 Mcg/kg/minute) and warm intravenous fluids (lactated ringers 10 ml/kg/hour) throughout the procedure. Immediately after anesthesia was administered, the subject was intubated to assure the airway remained unobstructed throughout the experiment. Heart rate, respiration, and oxygen saturation were monitored using a pulse oximeter. The body temperature of the subject was checked periodically and maintained with a Bair Hugger[®] (warm air circulating blanket). To minimize eye movements, a peribulbar injection of 1 cc Xylocaine, 4%, was administered just before beginning the laser radiation exposures. The eye was held open by a wire lid speculum and irrigated with 0.9% saline solution every few seconds throughout the procedure. Subjects were securely restrained in the prone position on a custom animal stage designed to allow for careful movements of an intubated subject in front of a Topcon TRC-50 \times fundus camera (Figure 4).

A Coherent Chameleon laser set to 834-nm wavelength pumped the Coherent Mira-OPO tuneable laser for the 1,110, 1,130, and 1,150 nm wavelengths used in this study. See Table 2 for a data-matrix with parameters of exposures. The bandwidth of the OPO laser ranged between 12 and 15 nm full-width at half max. A waveplate and an electronic shutter were used to control the power and exposure duration of the NIR laser at the corneal plane. A thin piece of glass placed slightly off axis just before the shutter was used to reflect a small portion of the NIR laser radiation to a Coherent power meter, PM3, read by a Coherent PowerMax 5000; this is referred to as the reference power meter. The OPO lased in TEM₀₀ mode with its Gaussian beam having a full-angle divergence and $1/e^2$ diameter at the corneal plane of 1.5 mrad and 4.8 mm, respectively, within the specifications by the manufacturer. A Melles Griot 633-nm HeNe laser was expanded and attenuated for use as a pointer to allow for careful placement of retinal lesions. A Spectra Physics 532-nm Millennia laser was used to place marker lesions to map a grid on the retina. A second electronic

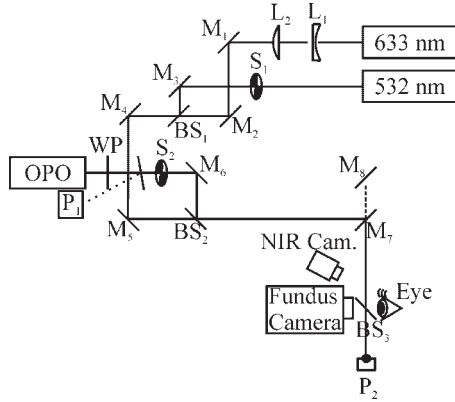


Fig. 4. The optical set-up. L1 and L2, lenses formed a $5\times$ beam expander for the 633-nm pointing laser; M1-5, broad-band visible mirrors; M6-8, silver mirrors. M7 and M8 formed a periscope to bring the beam up vertically to the viewing level of the fundus camera. BS1, a beam splitter which combined the two visible lasers; BS2 and BS3, identical beam splitters used to combine all three wavelengths; WP, waveplate. S1 and S2 were two independently controllable electronic shutters. P1, reference power meter; P2, photodiode connected to an oscilloscope; NIR Cam., near-infrared camera.

shutter controlled the delivery of the 532-nm laser radiation to the ocular plane. All three laser-wavelengths (NIR, 633, and 532 nm wavelengths) were co-aligned to deliver laser radiation to the ocular plane of the subject. The subject was placed such that its fundus was in focus and observable by a fundus camera by the scientific team (Fig. 4) with a 1-in. beam splitter placed just between the fundus camera's lens and the subject's eye. This beam splitter was highly transmissive in the visible allowing for a clear fundus image even during laser exposure. The total length of the optical train from the OPO laser head to the corneal plane was measured to be 261 cm.

With the OPO tuned to the desired wavelength, the alignment of the system was checked 24 hours and 30 minutes before the arrival of the subject. At these times, another Coherent power meter was placed at the corneal plane and the ratio of the reference power meter to the delivered corneal power was recorded. The ratio of the 532-nm laser radiation delivered to the corneal plane compared to the laser head setting was also obtained. These ratios were used to compute the power delivered to

TABLE 2. The Parameter Sets for NIR Exposures Investigated in This Study

λ (nm)	Exposure duration (ms)	$1/e^2$ diameter at corneal plane (mm)	Exposure location
1,110	100	4.8	P
1,130	100	4.8	P
1,150	100	4.8	P
1,319	80	5.0	M

P and M are for paramacula and macula, respectively.

the corneal plane and to ensure stability and repeatability of the experiments. To verify the proper exposure duration, a photodiode connected to an oscilloscope was placed perpendicular to the corneal plane. In addition to the photodiode, an Electro Physics NIR camera was placed off axis to zoom in on the corneal plane and recorded on a DVD. The NIR camera helped to confirm that the laser beam was not clipped by the subject's iris when delivering the NIR laser radiation. The fundus camera was equipped with a digital camera mounted to view the fundus in addition to a 35-mm film camera mounted in another position to take traditional photos. Fundus photographs were taken pre, 1 hour, and 24 hours post-NIR laser radiation exposure.

A set of 532-nm marker lesions using 48 mW at the corneal plane exposed for 20 milliseconds were made along the macula-paramacula boundary to map out a grid for referencing laser exposures in our data set. NIR laser radiation, all 100-millisecond exposures were then placed along the grid map in the paramacula. Subject's maculas were not available to use in the OPO study. The paramacula grid location and reference power meter reading were recorded. Three observers inspected the subject's retina for lesions at 1- and 24-hour end points. These "lesion/no lesion" data were processed in Probit analysis software to determine the estimated dose which causes damage 50% of the time, called an ED_{50} . The Probit analysis takes the binomial lesion/no lesion data forming the sigmoid dose-response curve and fits the data to a linear regression using a maximum likelihood algorithm. The Probit reveals information on the confidence intervals (CI) including the upper and lower fiducial limits (CI = 95%) and the ED_{50} (CI = 50%). Probit analysis has been reported by Cain and Noojin to provide the most suitable method for determining ED_{50} thresholds and is a well-known method for determining dose-response curves [21,22]. Slit lamp photographs were taken of subjects post-exposure. To check for any leakage from the placed lesions, fundus fluorescein angiography was performed and recorded using 35-mm film immediately following the 1- and 24-hour retinal lesion reads. The dose levels for fundus fluorescein angiography were 0.5–1 mg/kg IV (acepromazine) given 20 minutes prior to administering the Fluorescein (0.4 ml/subject) dye.

The exposures for the 1,319-nm laser radiation used a similar experimental technique, save for the laser source was a LEE-laser and the shutter was manufactured by nmLaser Products, Inc (San Jose; CA). Exposures at 1,319 nm were for 80 milliseconds to the macula of the same subjects used in the OPO experiment. The 1,319-nm beam characteristics at the corneal plane were a $1/e^2$ diameter of ~ 5 mm with a full-angle beam divergence of 13.3 mrad and M^2 of ~ 50 .

An estimated fit of the damage threshold data was performed using a scaling algorithm developed with the three fundamental criteria previously described. The scaling factor (SF) was created by breaking the fundamental criteria into a simple heat source term, S (W/cm^3), for a wavelength, λ , in the NIR based on

$$S(\lambda) = \frac{P}{\pi r^2} (\mu_a) \quad (2)$$

where P is the power reaching the retina (W), r is the $1/e^2$ radius of the beam at the retina (see Fig. 3), and μ_a is the linear absorption coefficients of the RPE (assumed to include water) in cm^{-1} . If an input is assumed to be unity at the corneal plane, then the power reaching the retina can be taken as the fraction of transmitted power, P_T , to the retina based on the results from Figure 1.

The simple heat source term, S , can be calculated for the NIR region using Equation (2), then divided into $S(1,110\text{ nm})$ to create the SF relative to the 1,110-nm damage threshold. Thus, the SF for the NIR is calculated by

$$\text{SF} = \frac{(P_{T,1110\text{ nm}}/r_{1110\text{ nm}}^2)}{(P_{T,\lambda}/r_\lambda^2)} \left(\frac{\mu_{a,1110\text{ nm}}}{\mu_{a,\lambda}} \right) \quad (3)$$

A fit to ED_{50} data in the NIR can then be made by multiplying the SF by the experimental 1,110-nm ED_{50} value.

RESULTS

The results of the Probit analysis of the yes/no data at 1 and 24 hours for each wavelength exposure for individual and grouped subjects are in Table 3. Probit results for combined subjects in Table 3 represent the complete Probit analysis performed on all the yes/no data obtained from the corresponding data set at the reported laser radiation wavelength. Probit analysis should not be confused as an average over all subjects. Slit lamp photography always appeared negative for lesions in the cornea, aqueous, and lens. The Gaussian-beam profiles had $1/e^2$ diameters of 4.8 and 5 mm for the OPO and LEE lasers, at the cornea, respectively. The OPO and LEE lasers' full-angle beam divergence were 1.5 and 13.3 mrad, respectively.

The 80-millisecond threshold exposure for the 1,319-nm laser radiation wavelength can be scaled to 100 milliseconds based on

$$\text{ED}_{50-100\text{ ms}}(\text{J}) = \text{ED}_{50-80\text{ ms}}(\text{J}) * \left(\frac{100}{80} \right)^{(3/4)} \quad (4)$$

where J are units of Joules, as reported in studies investigating the time-dependence relationship to maximum permissible exposure levels [23]. Using Equation (2), the SF from Equation (3), over several wavelengths is given in Table 4.

The 24-hour ED_{50} data in Table 3 are plotted in Figure 5 (all 1,319-nm data were scaled to 100 milliseconds using Eq. 4). A fit to the ED_{50} data in Figure 5 was made by multiplying the SF (Table 4) by the 24-hour ED_{50} value for combined subjects at 1,110-nm laser radiation (193-mW delivered to cornea).

Subject 1 was exposed to 1,150-nm laser radiation in the paramacula on two separate occasions; 3 weeks apart. The first set of exposures resulted in very large lesions (large at 1 hour, and even larger at 24 hours) with an ED_{50} of 406 mW, see Figure 6a, while the second set of exposures resulted in much smaller lesions (remained small at 1 and 24 hours) with an ED_{50} of 567 mW, see Figure 6b. Lesions labeled without numbers in Figure 6 are marker lesions used to reference the grid location of each NIR radiation

exposure on the fundus. Combining all yes/no data for both exposure sessions (data from both Figure 6a and b) gave the resulting ED_{50} of 439 mW reported in Table 3.

DISCUSSION

Based on fundus camera observation, all of the NIR retinal lesions in this study had the typical appearance of looking larger than the marker lesions produced by a 532-nm wavelength laser. At higher NIR power exposures, lesions commonly appeared larger than lesions from lower power exposures (Fig. 6a). Lesions always continued to grow over the 24-hour period with many lesions only becoming apparent at the 24-hour end point (Table 3). These observations are similar to those made by Zuclich et al. [5,9,24,25] who reported that the delayed onset inflammation is a characteristic of NIR laser-tissue interaction with the retina. We believe the retina's delayed response to NIR laser radiation threshold energy levels is related to the large beam diameter owing to chromatic dispersion and the strong increase in water absorption at these laser radiation wavelengths, resulting in a more uniformly distributed heating effect in the retina as compared to a localized effect due to strong RPE absorption at visible laser radiation wavelengths. In the study presented here, power levels that produced lesions never resulted in a retinal hemorrhage.

In regards to the 100-millisecond paramacular exposures to the 1,150-nm laser radiation, only one subject out of three tested yielded any funduscopically observable lesions. This single subject's 1-hour ED_{50} data were not statistically significant since the upper fiducial limit was greater than 50% of the corresponding ED_{50} . However, the 24-hour Probit of subject 1's 1,150-nm wavelength data set maintained the upper and lower fiducial limits within 50% of the ED_{50} . Subject 1's 24-hour ED_{50} 1,150-nm laser radiation threshold value of 439 mW (delivered to the cornea) was a power level of approximately 2.27 times greater than the 193-mW 24-hour ED_{50} from 1,110 nm. Based upon Figure 5, the 100-millisecond ED_{50} for 1,150-nm laser radiation is 1,181 mW, or a SF of ~ 6 times higher than the 1,110-nm 24-hour ED_{50} (Table 4), but the OPO laser was only capable of delivering up to ~ 870 mW, to the corneal plane. Subjects 2 and 3 were tested at the 1,150-nm laser radiation wavelength and yielded no funduscopically observable lesions on the retina. The 24-hour ED_{50} values followed the SF trend well for subjects 2 and 3 at 1,110, 1,130, and 1,319 nm laser radiation wavelengths and for subject 1 at 1,130 and 1,319 nm.

The SF method previously presented based on the three fundamental criteria creates a useful technique for fitting ED_{50} data to 100-millisecond exposures from NIR laser radiation. The SF method predicted the 1,319-nm laser radiation ED_{50} for combined subjects to be 15.3 W delivered at the cornea. This predicted value is only $\sim 12\%$ larger than the 24-hour ED_{50} experimental value of 13.7 W in Table 3 (experimental value was scaled to the 100-millisecond exposure using Eq. 4). This error is within the upper and lower fiducial limits of the 24-hour ED_{50} , 15.3 and 11.8 W, respectively (fiducial limits here were scaled

TABLE 3. Summary of the Data Obtained From the Retinal (P for Paramacula, M for Macula) Damage Thresholds

λ (nm)	Exp. dur. (milliseconds)	Loc.	Subj.	1 hour				24 hours						
				Yes	No	ED ₅₀ (mW)	Upper fiducial limit (mW)	Lower fiducial limit (mW)	Yes	No	ED ₅₀ (mW)	Upper fiducial limit (mW)	Lower fiducial limit (mW)	
1,110	100	P	2	14	21	170	197	171	171	17	18	161	172	148
			4	9	25	153	153	153	153	11	23	132	132	132
			3	8	19	376	147	310	310	14	13	299	373	215
1,130	100	P	2, 3, and 4	31	65	263	405	207	207	42	54	193	237	160
			3	6	29	412	1,150	370	370	11	24	364	457	318
			1	12	22	304	2,610,000	201	201	15	19	266	314	231
1,150	100	P	2	15	17	275	306	248	248	26	6	210	241	15.6
			1,2, and 3	33	68	346	501	295	295	52	49	270	301	241
			1	11	20	765	287	489	489	21	10	439	524	255
1,319	80	M	3	0	10	N/A	N/A	N/A	N/A	0	10	N/A	N/A	N/A
			2	0	5	N/A	N/A	N/A	N/A	0	5	N/A	N/A	N/A
			1, 2, and 3	11	35	N/A	N/A	N/A	N/A	21	25	872	872	872
1,319	80	M	1	11	15	15,900	18,200	13,600	13,600	18	8	12,500	14,200	9,580
			3	6	10	16,500	N/A	N/A	N/A	9	7	14,500	19,100	8,050
			2	8	15	23,700	28,200	20,200	20,200	13	10	19,800	23,300	15,800
			1,2, and 3	25	40	18,900	21,800	17,000	17,000	40	25	14,500	16,200	12,500

N/A entered for an ED₅₀ indicates no lesions were observed, even though exposures were at ~830 mW (maximum power available for 1,150 nm) for 100 milliseconds. N/A entered in a fiducial limit (FL) indicates the FL was unattainable for the relevant data set.

TABLE 4. The Scaling Factor, SF, From Equation (2), for Several Wavelengths in the NIR

λ (nm)	SF
1,100	0.872
1,110	1.000
1,130	1.563
1,150	6.119
1,200	12.299
1,250	12.343
1,300	27.899
1,315	60.267
1,319	79.696
1,320	85.898

The SF is intended to be multiplied by the 1,110-nm laser radiation wavelength's 24-hour ED₅₀.

to 100-millisecond exposures using Eq. 4), from the experiment (Table 3). The action spectrum produced by Lund et al. [14] shows that the expected ED₅₀ for 100 milliseconds, 1,110-nm laser radiation is approximately a little less than 200-mW power delivered to the cornea. Our experimental data from three subjects for 100 milliseconds, 1,110-nm laser radiation yielded an ED₅₀ of 193-mW power at the corneal plane, very close to the prediction made by Lund et al. [14]. The SF values presented here are based on the 1,110-nm reference of 193 mW delivered to the cornea. It should be stressed that the SF algorithm depends on relative values between wavelengths for percent transmission, absorption, and beam-waist radii delivered to the

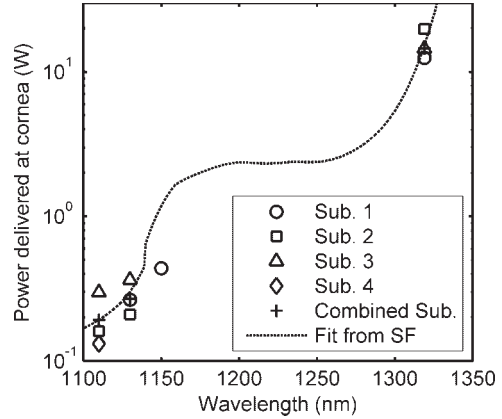


Fig. 5. The 24-hour, 100-millisecond, ED₅₀ retinal damage thresholds from Table 3 (1,319-nm data were scaled to 100 milliseconds by Eq. 4) and the SF fit determined by multiplying the SF values (Table 4) by the 1,110-nm ED₅₀ threshold for combined subjects.

retina and does not require absolute values. More advanced modeling methods are required to determine and understand absolute values and their relationship on retinal damage thresholds.

For the 1,150-nm wavelength, subject 1 was exposed to this laser radiation early on in the study, and brought in a second time 3 weeks later to determine if the 1,150-nm lesions were repeatable. In the first 1,150-nm exposure, at 1 hour, subject 1 had large lesions even at 500 mW of power delivered to the cornea and an 1,150-nm 24-hour ED₅₀ (from this first exposure set only) of 407 mW (see Fig. 6a). In

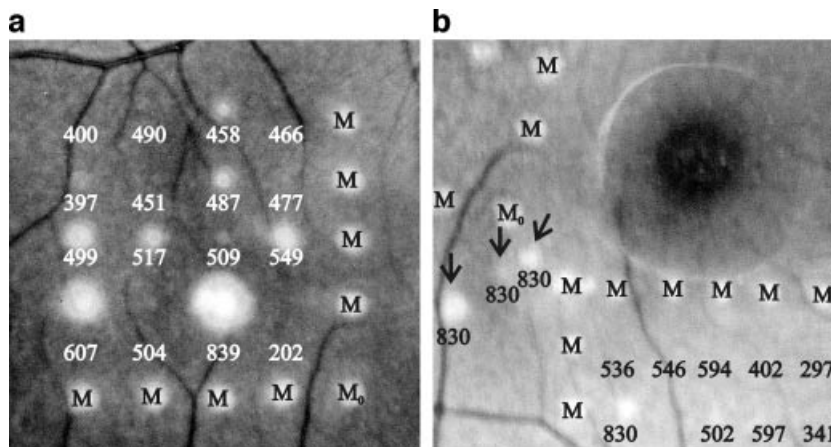


Fig. 6. Fundus camera images captured of subject 1 at 24-hour post-exposure to 1,150-nm laser radiation (fundus camera was set to 35° field of view in each image). The letter M denotes a marker lesion, with M₀ acting as a reference marker between a and b. The numbers marked below the grid locations represent the power (mW) delivered to the corneal plane for 100 milliseconds. **a:** Displays the large lesions observed for the first 1,150-nm exposure with a resulting ED₅₀ of 406 mW. **b:** Displays lesions observed for the second 1,150-nm exposure, conducted 3 weeks later, on the same eye resulting in an ED₅₀ of 567 mW. The arrows point to exposure areas off the marker grid in attempts to check experimental repeatability.

the second 1,150-nm exposure, the only 1-hour lesions were the 830-mW power levels delivered to the cornea giving much smaller visible lesions than the first data set with a resulting 1,150-nm 24-hour ED₅₀ (from this second exposure set only) of 567 mW (see Fig. 6b). The pigmentation of the two regions in the paramacula which were exposed to the 1150-nm laser radiation were noted to be fairly uniform and did not appear any lighter or darker than any other subject's paramacula.

The SF method predicts the ED₅₀ of 1,150-nm laser radiation (100-millisecond exposure) should be ~6 times greater (Table 4) than the 1,110-nm ED₅₀ (Fig. 5). Subject 1 yielded 1130 and 1319 nm ED₅₀ results consistent with the SF method (Table 3 and Fig. 5), suggesting absorptive properties of this subject's retina are not largely deviant from other subjects. Given these data trends and the fact that subject 1 had two very different ED₅₀'s over a 3-week interval for the 1150-nm exposure with remarkably smaller lesions on the second exposure, it is possible that the refractive state of subject 1's eye varied between exposures. Possible sources for causing this type of variation include the anesthesia to induce the relaxed state of the eye and ocular growth [16]. All subjects were checked for refractive error several months prior to beginning the damage threshold studies, but are not routinely checked. In addition, path length was never measured at any point in the study. Data for this subject suggest that it may be beneficial to routinely screen subjects before the start of an exposure, after the subject's eye is believed to be in a fully relaxed state, to check for consistency in refractive error and/or ocular path length.

CONCLUSION

The experimental ED₅₀ retinal thresholds for 100-millisecond exposures to laser radiation wavelengths at 1,110, 1,130, and 1,319 nm were determined to be 193, 270, and 13,713 mW of power delivered to the corneal plane, respectively. The experimental ED₅₀ retinal threshold for 100-millisecond exposures to laser radiation at the 1,150-nm wavelength was not achieved due to limitations on the availability of power from the laser source. The SF method allows for trends in the fundamental criteria of transmitted energy, retinal absorption, and refractive error to shape the fit, as opposed to exact values of these criteria, which are difficult to determine. Given that the ED₅₀ for 1,150-nm laser radiation was achieved on one subject, it may be worthwhile to routinely screen for refractive error and measure the ocular path length of subjects prior to beginning a NIR retinal threshold experiment. This would eliminate the uncertainty in the subject's path length or refractive error variability whether from growth or anesthesia.

ACKNOWLEDGMENTS

Support was provided by the Consortium Research Fellowship Program at the Air Force Research Laboratory under contract number FA8650-05-2-6501.

REFERENCES

1. ANSI. American National Standard for Safe Use of Lasers. Orlando, FL: Laser Institute of America; 2000.
2. ICNIRP. Revision of guidelines on limits of exposure to laser radiation of wavelengths between 400 nm and 1.4 microns. *Health Phys* 2000;79(4):431-440.
3. Vincelette RL, Rockwell BA, Thomas RJ, Lund DJ, Welch AJ. Thermal lensing in ocular media exposed to continuous-wave near-infrared radiation: 1150-1350 nm region. *J Biomed Opt* 2008;13(5):054005.
4. Zuclich JA, Lund DJ, Stuck BE, Edsall PR. Ocular effects and safety standard implications for high-power lasers in the 1.3-1.4 μm wavelength range. San Antonio, TX: Air Force Research Laboratory; 2004. Report no. AFRL-HE-BR-TR-2004-0187. pp. 1-16.
5. Zuclich JA, Schuschereba ST, Zwick H, Boppart SA, Fujimoto JG, Cheney FE, Stuck BE. A comparison of laser-induced retinal damage from infrared wavelengths to that from visible wavelengths. *Lasers Light Ophthalmol* 1997;8(1): 15-29.
6. Zuclich JA, Lund DJ, Stuck BE. Wavelength dependence of ocular damage thresholds in the near-IR to far-IR transition region: Proposed revisions to MPEs. *Health Phys* 2007;92(1): 15-23.
7. Lund DJ, Stuck BE, Beatrice ES. Biological research in support of project MILES. San Francisco, CA: Letterman Army Institute of Research; 1981. Report no. 96. pp. 1-54.
8. Lund DJ, Edsall P, Stuck BE. Ocular hazards of Q-switched near-infrared lasers. In: Stuck BE, Belkin M, eds. *Laser and Noncoherent Light Ocular Effects: Epidemiology, Prevention, and Treatment, III*. San Jose, CA: SPIE; 2003;85-90.
9. Zuclich JA, Zwick HT, Schuschereba ST, Stuck BE, Cheney FE. Ophthalmoscopic and pathologic description of ocular damage induced by infrared laser radiation. *J Laser Appl* 1998;10(3):114-120.
10. Cain CP, Noojin GD, Stolarski DJ, Thomas RJ, Rockwell BA. Near-infrared ultrashort pulse laser bioeffects studies. In: Defense Do, eds. *Volume AFRL-HE-BR-TR-2003-0029*. Air Force Research Laboratory; 2003.
11. Lund DJ, Edsall P. Action Spectrum for Retinal Thermal Injury. *Laser and Noncoherent Light Ocular Effects: Epidemiology Prevention and Treatment, III*. San Jose, CA: SPIE; 1999. pp 324-334.
12. Lund DJ, Edsall P, Stuck BE. Spectral dependence of retinal thermal injury. In: Exarhos GJ, Guenther AH, Kozlowski MR, Lewis KL, Soileau MJ, eds. *Laser-Induced Damage in Optical Materials*. San Jose, CA: SPIE; 2000. pp 22-34.
13. Lund DJ, Edsall P, Stuck BE. Wavelength dependence of laser-induced retinal injury. In: Manns F, Söderberg PG, Ho A, Stuck BE, Belkin M, eds. *Ophthalmic Technologies XV*. Bellingham, WA: SPIE; 2005. pp 383-392.
14. Lund DJ, Edsall P, Stuck BE. Spectral dependence of retinal thermal injury. *J Laser Appl* 2008;20:2.
15. Maher EF. Transmission and absorption coefficients for the ocular media of the Rhesus monkey: USAF School of Aerospace Medicine; 1978, September 15, 1974 to September 15, 1976. Report no. SAM-TR-78-32. pp 1-104.
16. Fernandes A, Bradley DV, Tigges M, Tigges J, Herndon JG. Ocular measurements throughout the adult life span of rhesus monkeys. *Invest Ophthalmol Vis Sci* 2003;44(6): 2373-2380.
17. Li G, Zwick H, Stuck B, Lund DJ. On the use of schematic eye models to estimate retinal image quality. *J Biomed Opt* 2000;5(3):307-314.
18. Westheimer G. The eye. In: Mountcastle VB, ed. *Including Central Nervous System Control of Eye Movements*. St. Louis, MO: C.V. Mosby Company; 1980. pp 482-503.
19. Gabel VP, Birngruber R, Hillencamp F. Visible and near infrared light absorption in pigment epithelium and choroid. In: Shimizu K, ed. *XXIII Concilium Ophthalmologicum* (Reprinted from the International Congress Series No. 450). Kyoto: Excerpta Medica, Amsterdam-Oxford; 1978. pp 658-662.

20. Birngruber R, Hillenkamp F, Gabel VP. Theoretical investigations of laser thermal retinal injury. *Health Phys* 1985;48(6):781–796.
21. Cain CP, Noojin GD. A comparison of various probit methods for analyzing yes/no data on a log scale. In: Defense Do, eds. Volume AL/OE-TR-1996-0102. Brooks City-Base, TX: USAF Armstrong Laboratory; 1996.
22. Finney DJ. Probit analysis. Cambridge, England: University Press; 1971.
23. Henderson R, Schulmeister K. *Laser Safety*. Philadelphia, PA: Institute of Physics Publishing; 2004. pp 132–220.
24. Zuclich JA, Lund DJ, Edsall PR, Stuck RE, Hengst G. Highpower lasers in the 1.3- to 1.4- μm wavelength range: Ocular effects and safety standard implications. In: Stuck BE, Belkin M, eds. *Laser and Noncoherent Light Ocular Effects: Epidemiology, Prevention, and Treatment*. San Jose, CA: SPIE; 2001. pp 78–88.
25. Zuclich JA, Schuschereba S, Zwick H, Cheney F, Stuck BE. Comparing laser-induced retinal damage from IR wavelengths to that from visible wavelengths. In: Stuck BE, Belkin M, eds. *Laser-Inflicted Eye Injuries: Epidemiology, Prevention, and Treatment*. San Jose, CA: SPIE; 1996. pp 66–79.